Journal of Ovonic Research Vol. 11, No. 1, January - February 2015, p. 11 - 20

THE STRUCTURE AND PROPERTIES OF $Nd_{0.66}(Sr_{1-x}Li_x)_{0.34}FeO_3$

S.A.GAD*, M. BOSHTA, AHMED F. MABIED, A.M. ABO EL-SOUD
Solid State Physics Department, National Research Center, El-Bohoos str., 12311Dokki, Giza,Egypt

$Nd_{0.66}(Sr_{1-x}Li_x)_{0.34}FeO_3$ series were synthesized using standard ceramic method. The properties of such materials were characterized by XRD and the results revealed that there are two phases; the major phase was neodymium iron oxide perovskite and the second phase was iron oxide. The crystal structure was refined by the Rietveld method using MAUD software. It was found that the fraction of neodymium iron oxide perovskite slightly decreases while the iron oxide phase increases with increasing Li concentration. The energy gap values of the samples have been calculated and it was found that it decreased as Li increased. The electrical conductivity increases with increasing both Li content and temperature. The activation energy has been calculated from the electrical conductivity and it was found that, it deceases with increasing Li content. The magnetic susceptibility shows non-linear variation with Li concentration.

(Received November 22, 2014; Accepted December 30, 2014)

Keywords: Structure, Optical, Electrical, Magnetic properties.

1. Introduction

Perovskite type metal oxides are widely studied both theoretically and experimentally due to very broad range of electrical properties from insulators to superconductors [1–5], metal to insulator transitions [6], magnetic properties [7], magneto-resistive properties [8,9], electrochemical and catalytic properties [10]. These properties make these materials important for numerous hi-tech applications such as solid oxide fuels cells [11–13], gas sensors, catalysis [14, 15], spin valves, magnetic field sensors [16], environmental monitoring applications [17] and spintronics devices [18].Solid oxide fuel cells (SOFCs) have been considered for long time as efficient devices for the direct conversion of the chemical energy of a fuel into electrical power, combining the benefits of environmentally friendly power generation with the advantage of fuel flexibility [19]. Conventional SOFCs used to operate at high temperatures (800–1000 °C) to maximize fuel conversion but this is also the origin of several long term problems, such as the interfacial reaction between the cathode and the electrolyte, and the degradation of the anode via particle coarsening.

Doping can bring about changes in conductivity, oxidation states, bond lengths, bond angles, lattice distortions, lattice parameters, phase transitions and controls the properties of any material. In the case of $AFeO_3$orthoferrites, (whereA¼ rear earth cation,e.g. La, Nd, Y, etc.), doping at A-site with alkaline earth metals (such as Ca or Sr) increases the electronic and ionic conductivities due to hole formation or formation of oxygen vacancies depending upon the synthesis conditions. In the past few decades much attention has been given to doped and undoped NdFeO3 orthoferrites and the effects of doping on the structural, electrical and magnetic properties have been investigated [20,21].

The characteristic of perovskite related ion oxides [22-24] are known to vary with the various heating conditions such as heating in air, oxygen or vacuum, maximum heating temperature, and cooling conditions like slowly cooling or quenching.

*Corresponding author: samiagad2000@yahoo.com

Because of essential properties of the perovskite related iron oxides like high electrical conductivity, existence of mixed valencies of transition metals and durability in alkaline bath, they can be used as sensors or electrode for electrocatalyst and photochemistry [25-27]. This work aims to study the effect of Li doping on the structural, optical, electrical and magnetic properties of $NdSrFeO_3$ prepared by solid state reaction.

2. Experimental

X-ray powder diffraction data were collected at ambient temperature in step scanning mode, using a computer controlled X-ray diffractometer ((PANalytical, Empyrean, Netherlands) with Cu k_α-radiation ($\lambda k\alpha$ = 1.5406 Å) operated at 30 mA and 45 kV. The powder diffraction patterns were scanned in the 2Θ range of 20–100°, with scan step 0.013 and counting time 20 s/step. Diffuse reflection measurements were done in the wavelength range from 300 nm to 1600 nm using Jasco (V-570) spectrophotometer. The A.C. conductivity was measured using a computerized LCR circuit type (Hioki 3532-50 LCR Hi-Tester, Japan) with frequency range 42 Hz - 5 MHz and over the temperature range from room temperature to 625 K. A vibrating sample magnetometer model 9600-1-VSM was used for the magnetic properties measurements.

3. Preparation

Polycrystalline $Nd_{0.66}$ $(Sr_{1-x}Li_x)_{0.34}$ Fe O_3 (where x = 0.05, 0.1, 0.2 and 0.3) samples were synthesized using standard ceramic techniques, using high purity (99.99%) Nd_2O_3, $SrCO_3$, Li_2CO_3 and Fe_2O_3 obtained from Sigma-Aldrich. To get a homogenous mixture, stoichiometric amounts of the starting materials were mixed followed by grinding. Circular pellets of 1.5 cm diameter and ~ 2 cm thickness were fabricated under pressure of 3 ton/cm^2. The mixtures of oxides and carbonates were heated in air first at 1000˚C and then at 1200˚C for 2 days with intermediate grindings. Heating rate was maintained at 5 ˚C/ min during sintering at each temperature, while all samples were cooled in closed off furnace.

4. Results and discussion

4.1. Structural

Figure (1) shows the collected powder patterns of $Nd_{0.66}$ $(Sr_{1-x}Li_x)_{0.34}$ FeO_3 (x = 0.05, 0.1, 0.2 and 0.3). The obtained powder profiles were analyzed using the PANalytical X'Pert High Score Plus package [28]. The patterns background, peak positions and integrated intensity of each peak were accurately determined before further analysis. The phase composition of the diffraction patterns were identified using the ICDD powder diffraction database (PDF-2, 2010) and search-match algorithm which included in the High Score Plus package. Rietveld quantitative analysis was performed using MAUD software [29]. The instrumental profile parameters were derived by the XRD data of a standard quartz sample.

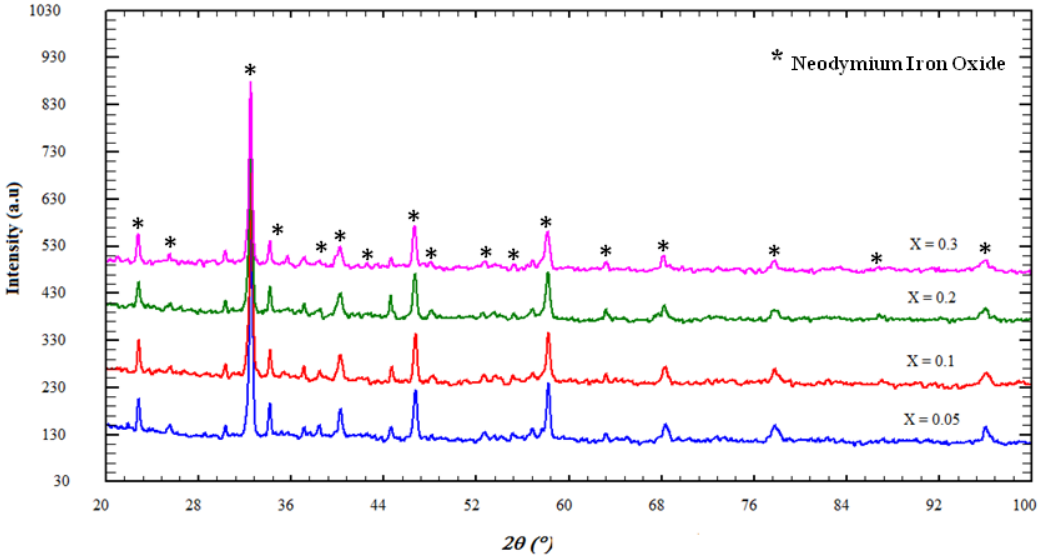

Fig.1 X-ray powder diffraction patterns of $Nd_{0.66}(Sr_{1-x}Li_x)_{0.34}FeO_3$.

The phase identification analysis by assigning the best-fitting of ICDD cards in both the relative intensity and peak position has revealed the formation of minor phase plus the main phase. The major phase was neodymium iron oxide perovskite structure matched with the ICDD (01-074-8963) and the second phase was iron oxide, according to the ICDD card (03-065-0390). Results of the Rietveld quantitative analysis with the reliability factors ($R_{wp}/R_p/S$**)** are given in table (1), also representative pattern of Rietveld quantitative refinement is shown in Fig. (2). It can be noticed clearly, that the fraction of neodymium iron oxide phase slightly decreases while the iron oxide phase increases with increasing the dopant concentration, which means that it needs higher energy in order to form the required phase.

Table 1 Rietveld quantitative results of the series $Nd_{0.66}(Sr_{1-x}Li_x)_{0.34}Fe\ O_3$,(x = 0.05, 0.1, 0.2 and 0.3).

X	$Nd_{0.66}(Sr_{1-x}Li_x)_{0.34}FeO_3$ %	Fe_2O_3 %	$R_{wp}/R_p/S$
0.05	98.85727	1.5298299	12 / 7 / 1.16
0.1	96.10497	3.8950262	13 / 7 / 1.18
0.2	95.05932	4.940685	12 / 7 / 1.11
0.3	76.67689	23.323112	15 / 6 / 0.99

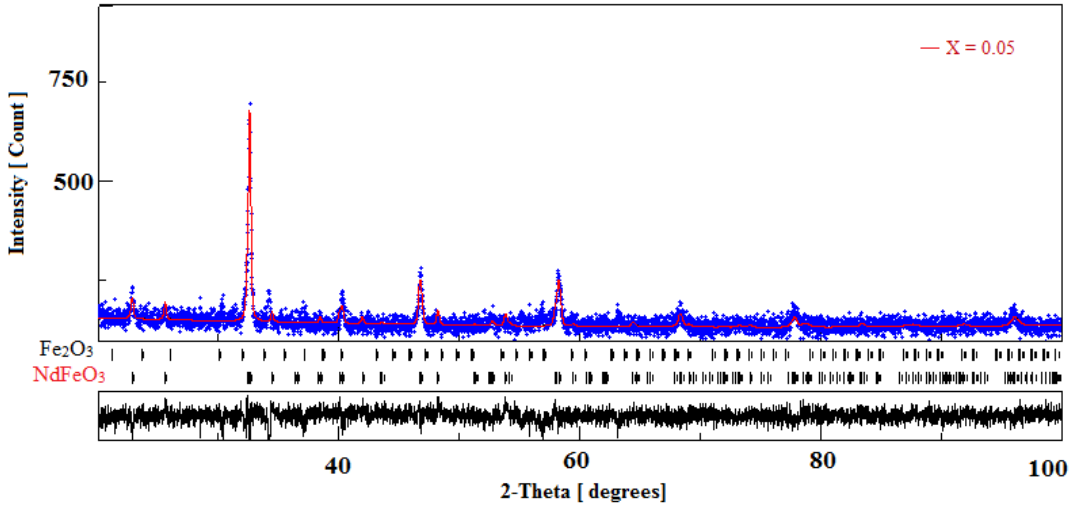

Fig.2 Representative Rietveld quantitative refinement plot of $Nd_{0.66}(Sr_{0.95}Li_{0.05})_{0.34}FeO_3$.

4.2. Optical Properties

Diffuse reflectance was carried out over the region 300-1600 nm at room temperature. The spectra within the entire frequency range are shown in Fig.(3). An examination of the shapes of the curves showed the striking resemblance among them. So it is reasonable therefore to conclude that the corresponding peaks are caused by the same transition mechanism in each material.

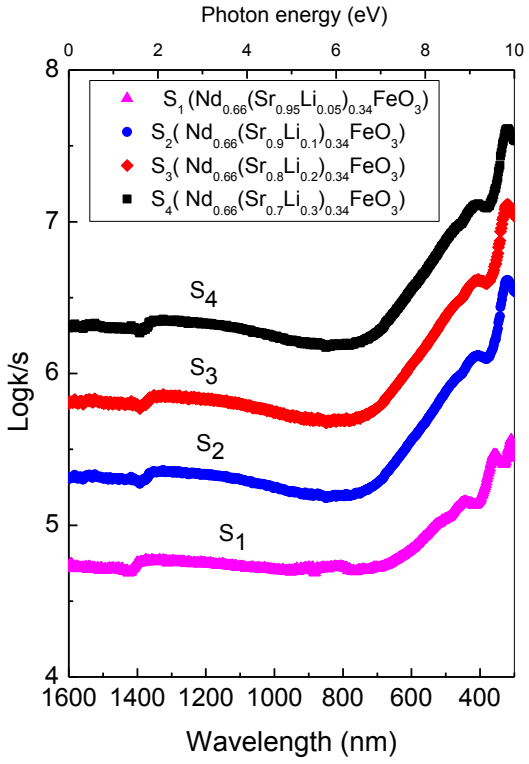

Fig.3 Log k/s versus the wavelength λ for $Nd_{0.66}(Sr_{1-x}Li_x)_{0.34}FeO_3$.

Discussing the absorption spectra obtained, there is an evidence of energy gap between the end of emission and the beginning of absorption. According to Tandon [30], the energy

coordination of the point on the low energy side of the curve at which the linear increase in (Log k/s) starts has been taken as the universal method for deducing the value of the forbidden energy gap. The values of the energy gap decrease with increasing the Li content as shown in Fig. (4), and tabulated in table (2).

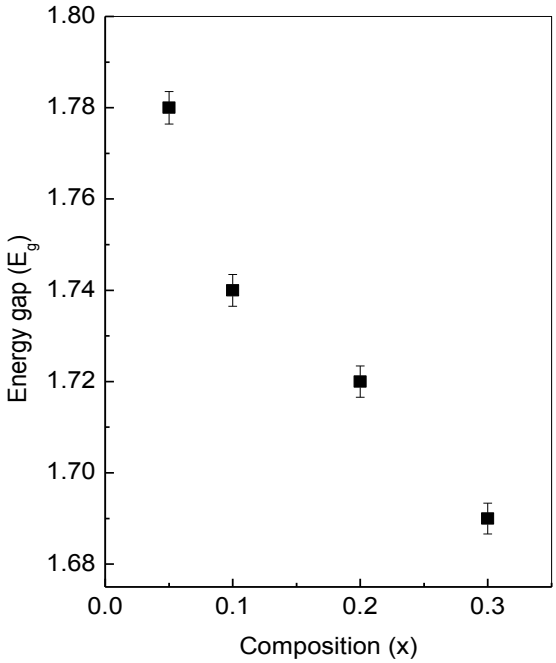

Fig.4 The optical energy band gap as a function of Li.

Table 2 The calculated values of the optical energy gap of $Nd_{0.66}$ $(Sr_{1-x}Li_x)_{0.34}$ FeO_3.

Composition (x)	Optical energy gap (eV)
0.05	1.91
0.1	1.76
0.2	1.72
0.3	1.69

4.3. Electrical Conductivity

The electrical conductivity (σ) of $Nd_{0.66}$ $(Sr_{1-x}Li_x)_{0.34}FeO_3$ series as a function of temperature in the range from 300 to 625 K is shown in Fig.(5a, 5b, 5c and 5d). The conductivity for the compositions increases with the temperature in this range showing semiconducting behavior. The linear variation of log (σ) with 1/T for all samples indicates that the conduction in these samples is through thermally activated process. The conductivity of the samples increases with increasing the composition parameter x, i.e. $Nd_{0.66}$ $(Sr_{1-x}Li_x)_{0.34}FeO_3$ might become more conducting with increasing Li content.

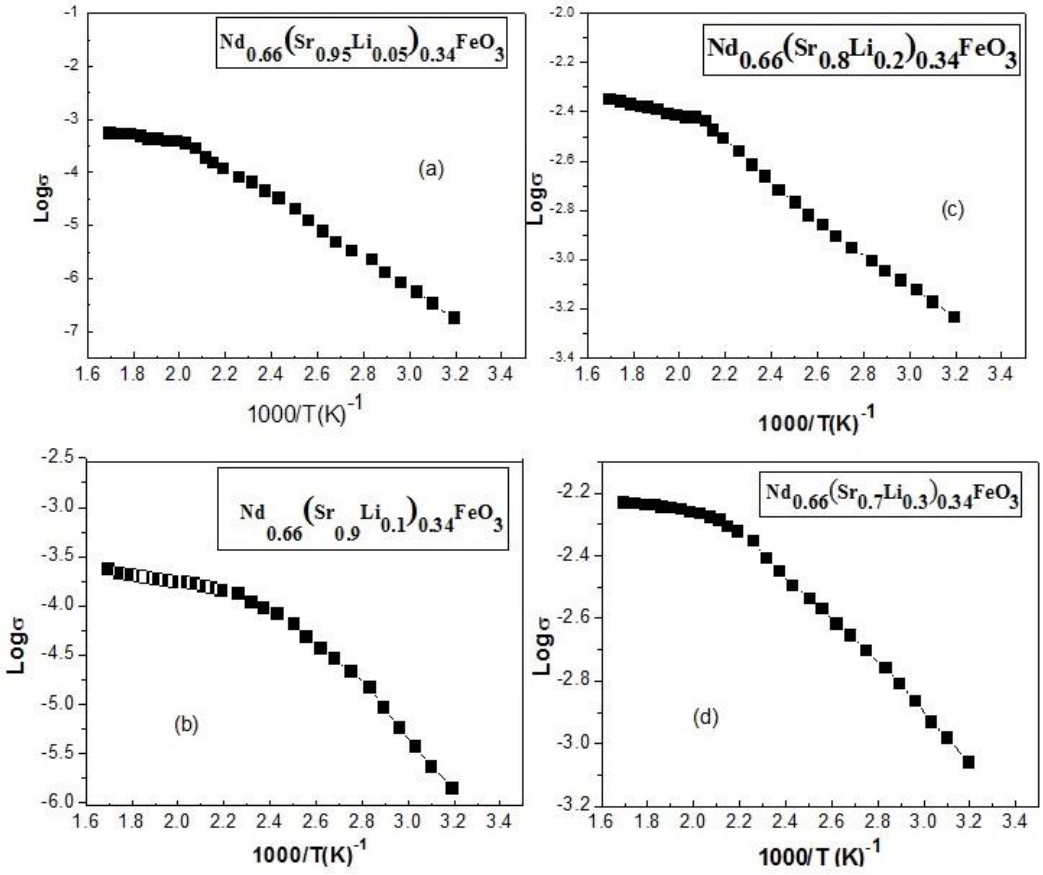

Fig.5 a,b,c,d: AC conductivity versus temperature for $Nd_{0.66}(Sr_{1-x}Li_x)_{0.34}FeO_3$.

The temperature dependence of the electrical conductivity can be expressed by:

$$\sigma = \sigma_0 \exp(-\Delta E/kT) \qquad (1)$$

in which ΔE is the activation energy , k is the Boltzman constant and σ_0 is the pre-exponential factor that contains several constants like the number of charge carriers and the average distance between Fe ions. It was found that the conductivity curves displayed a change in slope in the entire temperature range. It is known that neodymium ferrite experiences antiferomagnetic to paramagnetic transition with a Curie temperature of ~690K [31] and this is the probable reason for the change in slope [32]. According to Eq.1, one may expect two different regions of temperatures dependence with different slopes both could fit this relation [33]. The first lines are in low temperature region from 310 to 454-476 K, while the other lines are in the high temperature range from 454 to 476-592 K indicating a transition occur near 454- 476 K. The activation energies ΔE have been calculated from the slope of the lines in Fig.(5). In the lower temperature range, the activation energies decrease from 0.149 to 0.042 eV with increasing Li content. Also the activation energies in the higher temperature range decrease from 0.495 to 0.147 eV with increasing the Li content. The values of the activation energies are included in table (3).

Table 3 The calculated values of the activation energy from the electrical conductivity $Nd_{0.66}\ (Sr_{1-x}Li_x)_{0.34}\ Fe\ O_3$.

Composition (x)	Temperature range (K)	ΔE (eV)
0.05	310 - 476	0.495
	476 -591	0.149
0.1	313 -454	0.41
	454 -581	0.076
0.2	313 -463	0.15
	463-585	0.045
0.3	313- 471	0.147
	471-592	0.042

4.4. Magnetic properties

The magnetic hysteresis loops of $Nd_{0.66}\ (Sr_{1-x}Li_x)_{0.34}FeO_3$ powder have been measured as a function of Li concentration (x = 0.05, 0.1, 0.2 and 0.3) at room temperature which are shown in Fig.(6a,6b,6c and 6d). Table (4) confirmed that the magnetization M_s, coercivities H_c and Retentivity M_r depend on Li concentration. On the other hand, N.Hamed et al.[34] reported that the magnetization is reduced with increasing Li content for $Nd_{1-x}(Sr_{1-y}Li_y)_xMnO_3$. This behavior is very similar to that found in fixed valence substituted $La_{1-x}Ca_xMn\ (Fe/Ge)O_3$ and there it was ascribed to the reduction in the number of active Zener Mn^{3+} -Mn^{4+}bonds through the interference of the fixed valence sites Fe^{3+} or Ge^{4+} [35].

Table 4 The values of Magnetization M_s, *Coericivity* H_c *and Retentivity* M_r *of* $Nd_{0.66}\ (Sr_{1-x}Li_x)_{0.34}\ Fe\ O_3$.

x	(M_s)emu/g	(H_c) G	(M_r)emu/g
0.05	18.03	2239.4	9.114
0.1	23.1	1973.3	12.41
0.2	22.024	2411	10.960
0.3	23.993	1969.2	10.700

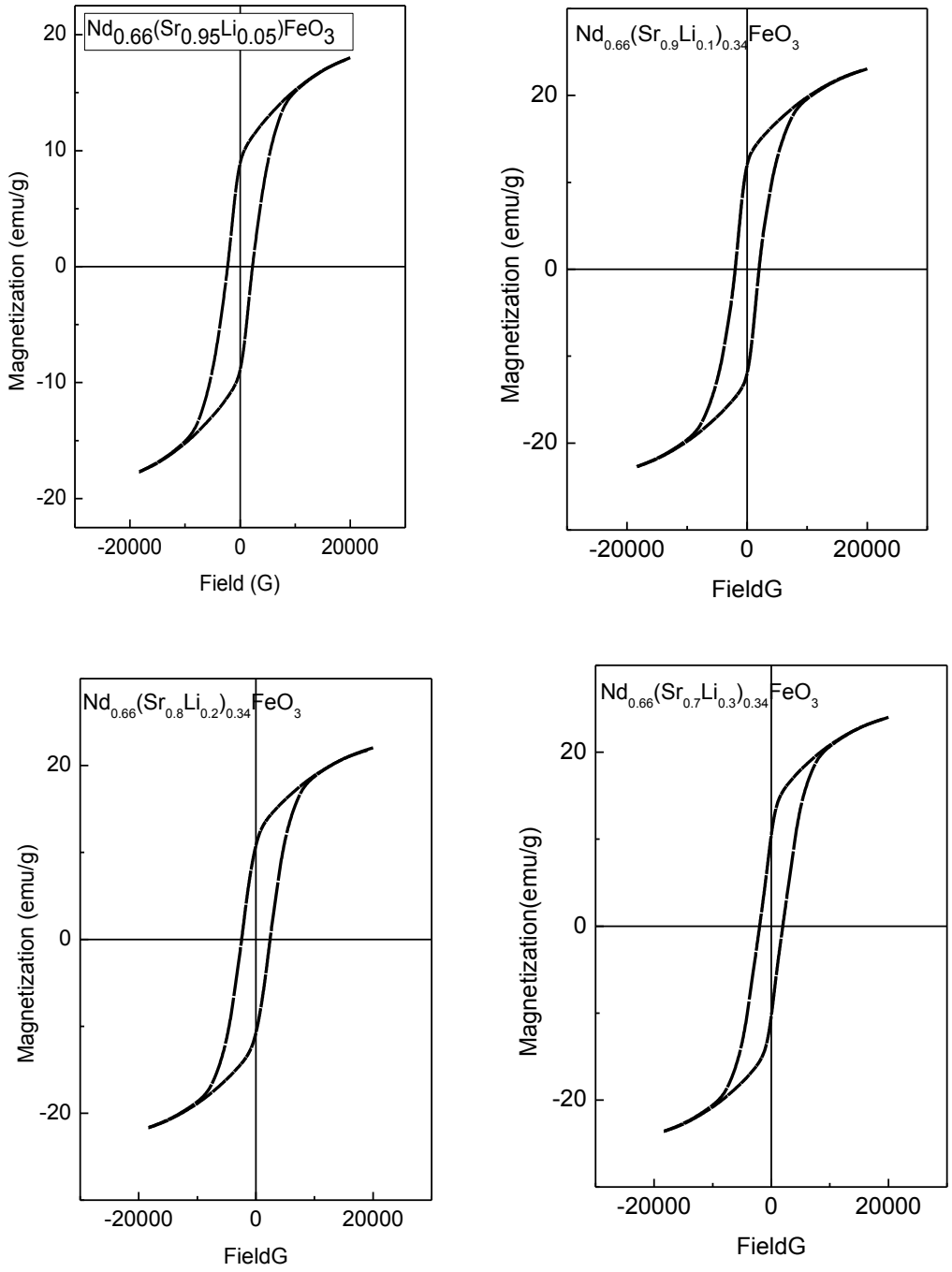

Fig. 6 a,b c,d The magnetic hysteresis of $Nd_{0.66}(Sr_{1-x}Li_x)_{0.34}FeO_3$ samples at room temperature.

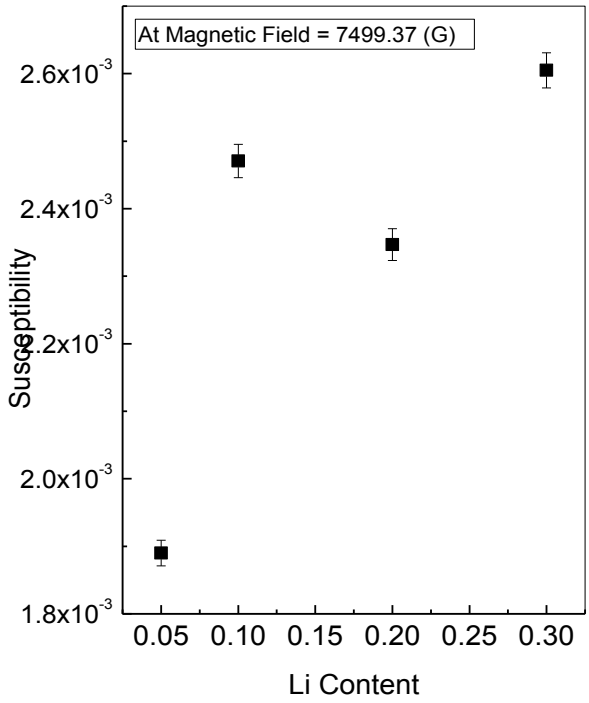

Fig. 7 Magnetic susceptibility versus Li concentration.

The magnetic susceptibility as a function of Li concentration is shown in Fig. (7). It is clear from this figure that the susceptibility shows non linear variation with the composition (x).

5. Conclusion

The crystal structure of $Nd_{0.66}$ $(Sr_{1-x}Li_x)$ $_{0.34}FeO_3$compounds was refined by the Rietveld method using MAUD software. It was found that the fraction of neodymium iron oxide perovskite slightly decreases while the iron oxide phase increases with increasing Li concentration. The energy gap was found to decrease with the increase of Li content. The electrical conductivity of the samples increases with increasing both of composition x and temperature. The activation energy calculated from the electrical conductivity and was found that it decrease with increasing Li content. The magnetic susceptibility shows non linear variation with the composition x.

References

[1] M .J Akhter, C. R. ACatlow,B Slater,A .M Walker,S Woodley.M,Chemistryof Materials**18** ,1552(2006).
[2] R .T .A Khan , M J Akhter,SolidStateCommunication**137**,110 (2006).
[3]J Zaanen,G. A Sawatzaky, J W Allen,PhysicalReviewLetters**55**, 418 (1985).
[4] J.GBendnorz,K.A Müller,PhysicaB: condensedMatter**64**, 189 (1986).
[5] G Binning,A Baratoff, H.EHonig,J.G Bednorz, PhysicalReviewLetters **45**, 1352 (1980).
[6] MImada, A Fujimori, YTokura,Metal-insulatortransitions,Physical Review Letters**70,** 1039 (1998).
[7] K Sreedhar,J. M Honig, MDarwin,M McElfresh,P. M Shand,J Xu, B.CCrooker,J Spalek, PhysicalReviewB**46**, 6382-6386 (1992).
[8] R.VHelmolt,J Wecker, BHolzapfel,L Schultz,K Samwer,PhysicalReview

Letters**71**,2321(1993).
[9] K Chahara, TOhno, MKasai,Y Kozono,Applied Physics Letters, **63**, 1990(1993).
[10] C.Y Park,F.V Azzarello, A. J Jacobson,JournalofMaterialChemistry**16**, 3624 (2006).
[11]N.Q Minh,Ceramicfuelcells,JournaloftheAmericanCeramicSociety**76**,563 (1993).
[12] H Ullmann,N Trofimenko, F Tietz,D Stöver,AAhmad-Khanlou,
Solid State Ionics**138**, 79 (2000).
[13] J Choi,J. H Lee,D. S Park, B.DHahn,W.H Yoon ,H Lin,Journalofthe
AmericanCeramicSociety**90**, 1926(2007).
[14]M.J Akhtar,Z.N Akhtar, J.PDragun,C.R.A Catlow, SolidStateIonics**104**, 147 (1997).
[15] H.J.M Bouwmeester,H Kruidhof, A. JBurggraf, SolidStateIonics**72,**185 (1994).
[16] Y.S Didosyan,H Hauser,V.Y Barash,P.L Fulmek,JournalofMagnetismand Magnetic
Materials**177**, 203 (1998).
[17] GMartinelli,M Carotta,M Ferroni,E Traversa,Sensors andActuators**B55**, 99 (1999).
[18] M.V Chetkin,Y.N Kurbatova,T. B Shapaeva,Journal of Magnetism and
MagneticMaterials**321**, 800(2009).
[19] S.C Singhal, K Kendaall, High Temperature Solid Oxide Fuel Cells:
Fundamentals, Design and Applications, **Elsevier, Oxford, UK**, (2003).
[20] N Dasgupta, R Krishnamoorthy, K.T Jacob,SolidStateIonics, **149,** 227(2002).
[21]A Bashir,M Ikram,R Kumar, P Thankur,K.H Chae, Journal ofPhysics:CondensedMatter
21, 325501 (2009).
[22] C. H Yo, E. SLee, andM. S Pyon, J. Solid State Chem.,**58**,411 (1988).
[23] G. Demazeau,Z LI-Ming, L Fournes, MPouchard, and PHagenmuller, J.Solid State Chem.,
72,31 (1988).
[24] F Menil, N Kinomura,L Fournes, J Portier, andP Hagenmuller, Phys.Stat. Sol.,
64, 261 (1981).
[25] J Hombo, J. Solid State Chem., **84**,138 (1990).
[26] YMatsmoto, J Kurimoto, and E Sato, J. Electronal. Chem.,**127**, 2360 (1980)
[27] Y Matsmoto, SYamada, T Nishida, andE Sato, J. Electronal.Chem.**102,**77 (1979).
[28]Scott SpeakmanA, PanalyticalX'PertHighScore Plus v3.0.
[29]L Lutterotti, M Bortolotti, G Ischia,I Lonardelli andH.-R Wenk,
"Rietveld texture analysis from diffraction images", Z. Kristallogr., Suppl. **26**, 125 (2007).
[30]S.P Tandon, J.P Gupta, Phys.Statusn Solidi, **38**,363 (1970).
[31] J.W Nielsen, Metall. Trans.**2**, 625 (1971).
[32] H.I Yoo, C.S Kim,Solid State Ionics,**53-56**, 583 (1992).[33]L.W Tai,M.M Nasrullah, H.U
Andersen, D.M Sparlin, S.R Sehlin, Solid State Ionics
76,259 (1995).
[34] NHamed,I El- Kassab, LHaupt,N Kasper,K Bärner, G.H Rao ,U.Sondermann,
EGmelin,Journal of Alloys and compounds**317-318**,145(2001).
[35] G.HRao,J.R Sun,AKattwinkel,L Haupt,K Bärner, E Schmitt,E Gmelin
Physica B**269**, 379(1999)**.**